Decreased *S100A9* expression alleviates *Clostridium perfringens* beta2 toxin-induced inflammatory injury in IPEC-J2 cells

Jie Li[1], Xiaoyu Huang[1], Kaihui Xie[1], Juanli Zhang[2], Jiaojiao Yang[1], Zunqiang Yan[1] and Shuangbao Gun[1,3]

[1] College of Animal Science and Technology, Gansu Agricultural University, Lanzhou, Gansu, China
[2] College of Life Sciences, Longdong University, Qingyang, Gansu, China
[3] Gansu Research Center for Swine Production Engineering and Technology, Lanzhou, Gansu, China

ABSTRACT

Background: S100 calcium-binding protein A9 (S100A9) is a commonly known pro-inflammatory factor involved in various inflammatory responses. *Clostridium perfringens* (*C. perfringens*) type C is known to cause diarrhea in piglets. However, the role of *S100A9* in *C. perfringens type* C-induced infectious diarrhea is unclear.

Methods: Here, the *S100A9* gene was overexpressed and knocked down in the IPEC-J2 cells, which were treated with *C. perfringens* beta2 (CPB2) toxin. The role of *S100A9* in CPB2 toxin-induced injury in IPEC-J2 cells was assessed by measuring the levels of inflammatory cytokines, reactive oxygen species (ROS), lactate dehydrogenase (LDH), cell proliferation, and tight junction-related proteins.

Results: The results showed elevated expression of *S100A9* in diarrhea-affected piglet tissues, and the elevation of *S100A9* expression after CPB2 toxin treatment of IPEC-J2 was time-dependent. In CPB2 toxin-induced IPEC-J2 cells, overexpression of *S100A9* had the following effects: the relative expression of inflammatory factors *IL-6*, *IL8*, *TNF-α*, and *IL-1β* was increased; the ROS levels and LDH viability were significantly increased; cell viability and proliferation were inhibited; the G0/G1 phase cell ratio was significantly increased. Furthermore, overexpression of *S100A9* reduced the expression of tight junction proteins in CPB2-induced IPEC-J2 cells. The knockdown of *S100A9* had an inverse effect. In conclusion, our results confirmed that *S100A9* exacerbated inflammatory injury in CPB2 toxin-induced IPEC-J2 cells, inhibited cell viability and cell proliferation, and disrupted the tight junctions between cells. Thus, decreased *S100A9* expression alleviates CPB2 toxin-induced inflammatory injury in IPEC-J2 cells.

Corresponding author
Shuangbao Gun,
gunsbao056@126.com

INTRODUCTION

Piglet diarrheal disease has seriously affected the economic growth of the pig production industry worldwide. Piglets are highly susceptible to enteritis caused by *Clostridium perfringens* (*C. perfringens*) type C, with a morbidity rate of 100% in infected piglets (*Posthaus et al., 2020*), and the pathogenicity of this pathogen is mainly mediated by the production of multiple toxins (*Forti et al., 2020*), among which *C. perfringens* beta (CPB) toxin produced by *C. perfringens* type C is the leading cause of intestinal inflammation (*Garcia et al., 2012*). *C. perfringens* beta2 (CPB2) is one of the major pathogens of CPB (*Schumacher et al., 2013*), the original first isolation of CPB2 was from a porcine enteritis strain in 1997 (*Gibert et al., 1997*). Therefore, the toxin is highly prevalent and can be isolated in piglets with enteritis and diarrhea (*van Asten, Nikolaou & Gröne, 2010*). It causes fatal enteritis (*Schumacher et al., 2013*) and plays a crucial role in *C. perfringens* pathogenicity (*Nagahama et al., 2015*; *Uzal et al., 2010*). In addition, the CPB2 toxin was highly cytotoxic to HL60, IPEC-J2 and porcine endothelial cells (*Gao et al., 2020*; *Gurtner et al., 2010*; *Nagahama et al., 2003*). Currently, the molecular mechanism of mRNAs in CPB2 toxin-induced damage in IPEC-J2 cells is unclear. Therefore, further genetic analysis is required to identify relevant genes to improve piglets' ability to resist diarrhea.

S100A9, also known as myeloid-related protein-14 (Mrp14), is a member of the S100 protein family and is an essential pro-inflammatory factor (*Huang et al., 2019a*; *Jhang et al., 2016*; *Källberg et al., 2012*). The protein has been demonstrated to regulate inflammatory responses in multiple cell types and is reported to be up-regulated in various cancer and inflammatory responses (*Lee et al., 2017*; *Markowitz & Carson, 2013*; *Vogl et al., 2007*). In addition, the *S100A9* gene has been reported to perform many biological functions, such as regulating cell proliferation, inducing apoptosis, influencing the migration of inflammatory cells, and activating cell surface receptors (*Shabani et al., 2018*). S100A9 interactions with other proteins affect the course of virus-induced innate immune responses (*Darweesh et al., 2018*). *S100A9* can bind to receptors such as TLR4 to activate multiple pro-inflammatory signaling pathways, resulting in an immune response generated by inflammatory factors associated with cell proliferation and inflammatory responses (*Kwon et al., 2013*; *Pandolfi et al., 2016*; *Shabani et al., 2018*). Another study demonstrated the reduced prevalence of inflammatory responses to knocking down the expression of *S100A9* has also been reported (*Abers et al., 2021*; *Zhao et al., 2021*). The *S100A9* gene is also involved in the inflammatory immune response caused by a bacterial infection in mammals (*Chen et al., 2009*). *S100A9* may also play a role in the immunological response to diarrhea caused by *C. perfringens* type C infection, although the exact mechanism is unknown. In a previous study by this research group, the *S100A9* gene was found to play an important role in *C. perfringens* type C diarrheal disease in piglets (*Huang et al., 2019b*), but the mechanism by which the *S100A9* gene regulates *C. perfringens* resistance in piglets is unknown. IPEC-J2 cells are porcine intestinal columnar epithelial cells that were isolated from newborn piglet jejunum, which are often used as an ideal model for studying pathogenic microorganisms (*Brosnahan & Brown, 2012*; *Liu et al., 2010*). In this study, the role of *S100A9* in the immune response has been

investigated by overexpressing and interfering with *S100A9* in CPB2 toxin-induced IPEC-J2 cells. This study's results provide a theoretical basis for further investigations of the molecular regulatory mechanisms of *S100A9* in *C. perfringens* type C diarrheal disease in piglets.

MATERIALS AND METHODS

Ethics statement

The animal experiments were conducted in strict accordance with the regulations of the Administration of Affairs Concerning Experimental Animals (Ministry of Science and Technology, China; revised in June 2004). and had been approved by the Institutional Ethic Committee of Gansu Agricultural University (Approval No. GAU-LC-2018-054). Animals were humanely sacrificed to alleviate suffering.

Cell and tissue sample collection

The piglets were purchased from Xitai Co., Ltd. in Dingxi, Gansu, China, and raised under the same environmental conditions with natural light and free access to food and water. Thirty seven-day-old piglets (Landrace × Yorkshire) of similar size and weight and in healthy condition were selected. Following the study of *Huang et al. (2019b)*, 25 piglets were randomly selected to receive 1 mL of 1×10^9 CFU/mL *C. perfringens* type C medium orally, and the remaining five piglets were inoculated with 1 mL of sterile medium as a control group, The experiment was conducted for five days. *C. perfringens* type C strain (CVCC 2032) was purchased from the Veterinary Culture Collection Center (Beijing, China). The culture medium was prepared as we described previously (*Huang et al., 2019b*). Test piglets were divided into control, susceptibility and resistance groups according to the piglet fecal scoring method described previously (*Huang et al., 2019c*; *Yang et al., 2013*). After slaughtering under barbiturate anesthesia, the heart, liver, spleen, lung, kidney, duodenum, jejunum and ileum tissues were collected and rapidly frozen and preserved in liquid nitrogen. The porcine IPEC-J2 cell lines were provided by Beina Biotechnology (Beijing, China).

Cell culture

All cells were cultured in Dulbecco's modified Eagle's medium (DMEM; HyClone, Logan, UT, USA) media supplemented with 10% fetal bovine serum (FBS) (HyClone, Logan, UT, USA) and 1% penicillin-streptomycin solution (Gibco, Carlsbad, CA, USA). Cells were incubated at 37 °C in a 5% CO_2 atmosphere. When the cell confluency reached 80%, 0.25% trypsin solution was used to detach and subculture the cells.

Transfection and CPB2 toxin treatment

The cell suspension were seeded into plates and transfected when the cells reached a confluency of 70%–80%. Then, referring to the instructions provided in the Lipofectamine® 2000 Reagent (Invitrogen, Carlsbad, CA, USA) manual, chemically synthesized *S100A9* inhibitor negative control (si-NC), *S100A9* inhibitor (si-*S100A9*), mRNA overexpression empty vector (pcDNA3.1), *S100A9* overexpression vector

Table 1 The information of interference RNA sequence.

Vector name	Sense (5′-3′)	Antisense (5′-3′)
si-NC	GGGAUGAGAAAGCCAUAAATT	UUUAUGGCUUUCUCAUCCCTT
si-S100A9	UUCUCCGAACGUGUCACGUTT	ACGUGACACGUUCGGAGAATT

(pc-*S100A9*) were transfected into IPEC-J2 cells and cultured for 24 h, for the knockdown and overexpression of *S100A9*. Finally, the cells were incubated with 20 μg/mL CPB2 toxin for 24 h, and the CPB2 toxin was prepared, purified, and used in doses according to our previous method (*Gao et al., 2020*; *Luo et al., 2020*). The *S100A9* overexpression vector was constructed from the pcDNA3.1 cloning vector, with 5′ NheI and 3′ XhoI as cloning sites. It was named pc-*S00A9* and was synthesized by GENEWIZ Life Sciences Company (Suzhou, China). Both *S100A9* inhibitor negative control (si-NC) and *S100A9* inhibitor (si-*S100A9*) were manufactured by Limibio (Hefei, China). The information on interference RNA is shown in Table 1.

Real-time quantitative PCR (RT-qPCR)

The total RNA was extracted from tissues and cells utilizing TRIzol (TransGen Biotech, Beijing, China) reagent according to the instructions provided in the kit. cDNA was synthesized using the Evo M-MLV reverse transcription master mix kit (Accurate Biotechnology, Hunan, China). RT-qPCR was carried out on a LightCycler 480II instrument (Roche, Basel, Switzerland) with SYBR® Green Premix Pro Taq HS qPCR Kit (Accurate Biotechnology, Hunan, China). The RT-qPCR reaction volume was 20 μL and contained the following: 2×Universal Blue SYBR Green qPCR Master mix-10 μL, Forward and Reverse primers-0.8 μL, cDNA-2 μL, ddH$_2$O-6.4 μL. The RT-qPCR reaction conditions were the following: pre-denaturation at 95 °C for 30 s, denaturation at 95 °C for 5 s, annealing at 60 °C for 30 s, 40 cycles. There were three replicates for each group, and the relative expression was calculated using the $2^{-\Delta\Delta Ct}$ method (*Livak & Schmittgen, 2001*). The relative expression of the mRNA used was calculated with *GAPDH* as the internal reference. The reaction primers were synthesized by Qingke Biotechnology (Beijing, China). The primer information is shown in Table 2.

Cell viability analysis

Cells were seeded into 96-well plates to assess the effect of *S100A9* on CPB2 toxin-induced IPEC-J2 cell viability. The cells were transfected when they reached 70%–80% confluence. After transfection for 24 h, the cells were incubated with 20 μg/mL CPB2 toxin for 24 h. After 24 h, 10 μL cell counting kit-8 (CCK-8) (Beyotime, Shanghai, China) solution was added to every well and incubated for 1 h at 37 °C in a 5% CO$_2$, 95% O$_2$ incubator. Next, the absorbance of the wells was measured at 450 nm with a microplate reader.

Inflammatory cytokine protein concentration detection

After transfection and toxin treatment (for 48 h), the supernatant of the treated cells was collected and centrifuged at 2,500 rpm for 20 min, and the supernatant was taken for use in

Table 2 A list of the primers used in the RT-qPCR.

Gene name	Transcript no.	Primer sequences (5′-3′)	Length (bp)
S100A9	NM_001177906.1	F: GGGACACCCTGAACCAGAAA	193
		R: TCCTCGTGAGAAGCTACCGT	
IL6	NM_001252429.1	F: AACCTGAACCTTCCAAAAATGG	90
		R: ACCGGTGGTGATTCTCATCA	
IL8	NM_213867.1	F: CTGCAGCTCTCTGTGAGGCTGC	199
		R: TCCTTGGGGTCCAGGCAGACC	
TNFα	NM_214022.1	F: GCACTGAGAGCATGATCCG	161
		R: AACCTCGAAGTGCAGTAGG	
IL-1β	XM_021085847.1	F: TGATGCCAACGTGCAGTCTA	92
		R: GGAGAGCCTTCAGCATGTGT	
ZO-1	XM_021098827.1	F: TGAGTTTGATAGTGGCGTTG	298
		R: TGGGAGGATGCTGTTGTC	
OCLN	NM_001163647.2	F: TCCTGGGTGTGATGGTGTTC	144
		R: CGTAGAGTCCAGTCACCGCA	
CLDN12	NM_001160079.1	F: ATGACGTCCGTTCTGCTCTT	101
		R: TACGTATGCATGCTGGGAGG	
GAPDH	NM_001206359.1	F: AGTATGATTCCACCCACGGC	139
		R: TACGTAGCACCAGCATCACC	

ELISA. Next, the samples were tested using ELISA Kits (Mlbio, Shanghai, China) according to the manufacturer's instructions. Finally, the OD values were measured at 450 nm using a microplate reader. Then, the standard curve was plotted, and the sample concentrations were calculated and reported in pg/mL.

Reactive oxygen species (ROS) detection

The amount of ROS in the samples was measured using a ROS assay kit (Solarbio, Beijing, China). The transfected and inoculated cells were collected and suspended in a DCFH-DA (2′,7′-Dichlorodihydrofluorescein diacetate) diluent (10 µmol/L) and incubated at 37 °C, 5% CO_2 cell incubator for 20 min. To ensure that the cells interact well with DCFH-DA, the cells were mixed by inversion for 3 min, followed by centrifuging at 1,500 rpm for 5 min. The supernatant was discarded, and the excess DCFH-DA was washed with PBS. Next, each experimental group used a fluorescence microplate reader to detect the fluorescence intensity of DCFH-DA. The DCFH-DA fluorescence intensity was directly proportional to the ROS levels in the IPEC-J2 cells.

Lactate dehydrogenase (LDH) activity assay

The cell supernatant was aspirated after treatment and then centrifuged at 3,500 rpm for 20 min. The activity of LDH in the IPEC-J2 sample was determined by using lactate dehydrogenase detection kits (Jancheng Bioengineering Institute, Nanjing, China).

EdU (5-ethynyl-2′-deoxyuridine) detection of IPEC-J2 cell proliferation

The number of EdU-positive cells was measured to assess the effect of the *S100A9* gene on CPB2 toxin-induced IPEC-J2 cell proliferation. The collected IPEC-J2 cell suspension was seeded into a 24-well plate and cultured for 24 h. Next, si-NC, si-*S100A9*, pcDNA3.1, and pc-*S100A9* were transfected into IPEC-J2 cells for 24 h using Lipofectamine® 2000. After treatment with 20 µg/mL CPB2 toxin for 24 h, IPEC-J2 cells were incubated with EdU (10 µM) working solution for 2 h (BeyoClick™ EdU-555 Cell Proliferation Assay Kit; Beyotime, Shanghai, China). The nuclei were stained with Hoechst 33342. Qualitative detection was performed using an inverted fluorescent microscope (Olympus, Japan).

Flow cytometry cycle analysis

After digestion with 0.25% trypsin, IPEC-J2 cells were collected, resuspended in pre-chilled 75% ethanol, and incubated overnight at 4 °C. Next, 2 µL of 10 mg/mL RNAseA was added to the IPEC-J2 cell samples to remove RNA at 37 °C for 30 min. This step was followed by adding 100 µL of 100 µg/mL PI (propidium iodide staining) solution and incubating for 10 min in the dark. Finally, the IPEC-J2 cell samples were detected by a flow cytometer (CytoFLEX, Beckman, CA, USA). Modfit (Verity Software House, Topsham, ME, USA) software was used to analyze the cell cycle distribution data.

Western blot analysis

The protein from IPEC-J2 cells was collected using radioimmunoprecipitation assay (RIPA) lysate containing 1% phenylmethanesulfonyl fluoride (PMSF). The protein content was determined by utilizing BCA (Bioss, China) protein detection kit. After denaturation, the protein samples were loaded for electrophoresis on an 8% SDS-PAGE gel. The voltages used to run the stacking gel, and the separation gel were 75 and 120 V, respectively. The transferred membrane was blocked by shaking in 5% skim milk (0.5% TBST) at 37 °C for 1 h. The membranes were then incubated with S100A9 antibody (1:1,000; PROGEN, Heidelberg, Germany) or β-actin antibody (1:1,000; Bioss, China) dilution overnight at 4 °C. Next HRP-labeled goat anti-mouse secondary antibody (1:1,000; Servicebio, Wuhan, China) was added and incubated for 30 min. After washing three times with TBST on a decolorizing shaker, the membranes were exposed to a chemiluminescence detection system (Fusion FX; VILBER, Collégien, France). Data was collected, and the quantitative analysis was performed with ImageJ (v1.8.0) software.

S100A9 protein-protein interaction (PPI) network prediction

The String (*Gan et al., 2015*) database was used, and evidence was chosen as the meaning of network edges to evaluate the interaction between S100A9 and other proteins. At the same time, *Sus scrofa* was selected as a control organism to predict the medium confidence (0.400) level. The prediction result data were exported to create the protein-protein interaction (PPI) networks between S100A9 and other proteins using Cytoscape (V3.8.0). Betweenness Centrality (BC) was used as a measure. The tightly linked clusters in the PPI network were analyzed to explore the functional clusters using MCODE in Cytoscape software, which clusters play major roles in the PPI networks.
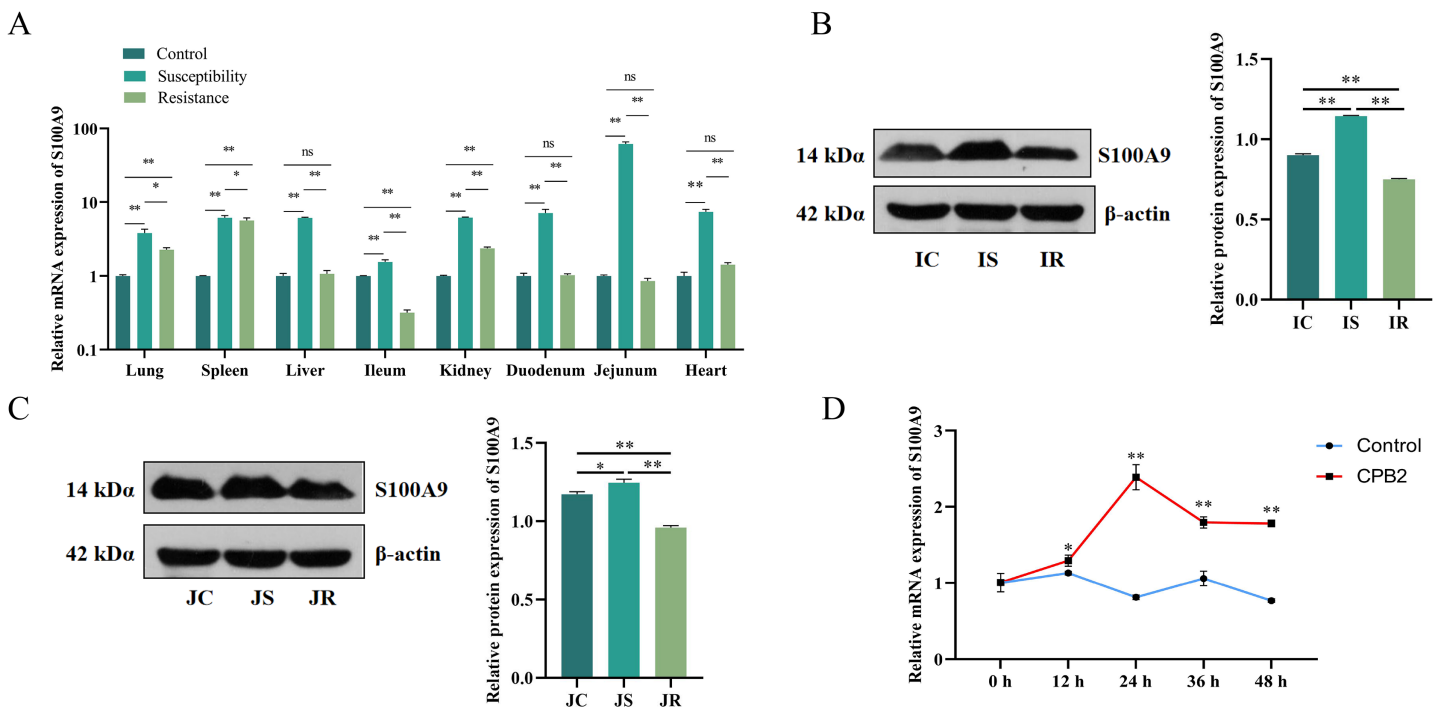
Figure 1 The level of expression of *S100A9* in tissues and IPEC-J2 cells. (A) The relative mRNA expression of *S100A9* in different tissues of each group. The control group represents healthy piglets, susceptibility group represents *C. perfringens* type C susceptible piglets and the resistance group represents *C. perfringens* type C resistant piglets. (B) Protein expression of S100A9 in ileum tissue in the control (IC), susceptibility (IS), and resistance (IR) groups. (C) Protein expression of S100A9 in jejunum tissue in control (JC), susceptibility (JS), and resistance (JR) groups at the protein level. (D) Relative mRNA expression of *S100A9* in IPEC-J2 after different treatment intervals of CPB2 toxin. *$P < 0.05$, **$P < 0.01$, ns implied $P > 0.05$.

Statistical analysis

Data analysis was performed using SPSS19.0.The student's t-test was used for comparison between the two groups. GraphPad Prism 8.0 (GraphPad Inc., La Jolla, CA, USA) software was used for plotting the data. All experiments were repeated thrice. Data are shown as mean ± SD. *$P < 0.05$ and **$P < 0.01$ indicate statistically significant differences.

RESULTS

Characterization of *S100A9* expression in tissues and cells

The *S100A9* expression profile and the cellular level were analyzed to investigate the effect of *S100A9* on CPB2 toxin-induced inflammatory injury in IPEC-J2 cells. First, RT-qPCR was used to detect the expression characteristics of *S100A9* in each treatment group of eight tissues. The results indicated that *S100A9* was significantly differentially expressed in the susceptibility group ($P < 0.05$), especially in the intestinal tissues (Fig. 1A). Further, the examination of the protein levels in the ileum and jejunum tissues (*i.e.*, the tissues that are closely associated with diarrhea in piglets) by Western blot. The results showed that S100A9 was significantly increased in both IS and JS groups ($P < 0.01$) (Figs. 1B, 1C and S1). The Western blot results indicated that the *S100A9* gene is closely associated with the immune response to *C. perfringens* type C infection. Next, the expression of *S100A9* was examined in different time intervals of CPB2 toxin treatment in IPEC-J2 cells. The results
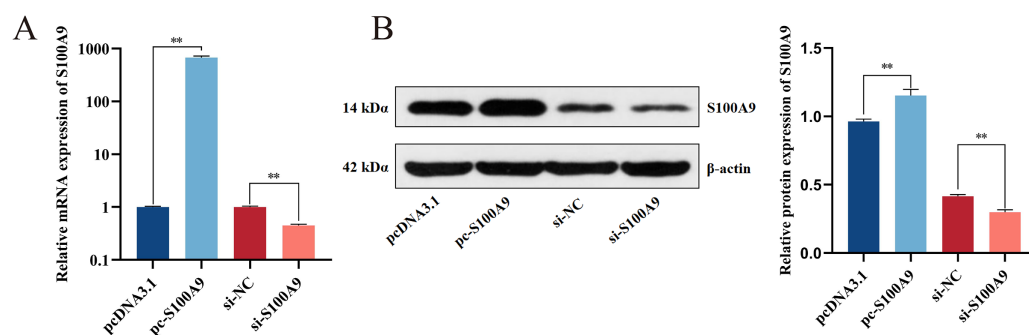
Figure 2 Detection of transfection efficiency of *S100A9*. (A) Relative mRNA expression of *S100A9*. (B) Protein expression of S100A9. $^*P < 0.05$, $^{**}P < 0.01$.

showed that CPB2 toxin significantly induced IPEC-J2 injury starting from 12 h. The expression of *S100A9* was up-regulated in a time-dependent manner and peaked at 24 h of CPB2 treatment after expression stabilized (Fig. 1D). Thus, these results indicated that *S100A9* might play a key in CPB2 toxin-induced IPEC-J2 injury.

Determining the efficiency of transfection

Chemically synthesized pcDNA3.1/pc-*S100A9* and si-NC/si-*S100A9* were transfected into IPEC-J2 cells. The expression of *S100A9* was detected with RT-qPCR and Western blot after transfection for 24 h. From both mRNA and protein levels, the results confirmed an extremely significant increase in the expression level of S100A9 after transfection with pc-*S100A9* compared with the pcDNA3.1 ($P < 0.01$). Further, expression levels of S100A9 were extremely significantly decreased after transfection with si-*S100A9* compared with the si-NC ($P < 0.01$) (Figs. 2A, 2B and S1), *i.e.*, overexpression and interference is success.

S100A9 up-regulates the CPB2-induced expression of inflammatory factors in IPEC-J2

RT-qPCR results showed that the expression of *IL-6*, *IL8*, *TNF-α* and *IL-1β* in IPEC-J2 cells induced by CPB2 toxin was significantly increased after overexpression of *S100A9*. ($P < 0.01$). On the other hand, the expressions of *IL-6*, *IL8*, *TNF-α*, and *IL-1β* were extremely significantly decreased in the CPB2 toxin-induced IPEC-J2 cells under interfering with *S100A9* ($P < 0.01$) (Fig. 3A–3D). Further, ELISA was used to detect the levels of inflammatory factors IL-6, IL8, TNF-α, and IL-1β in cell supernatant, the expression level of IL-6, IL8, TNF-α, and IL-1β were significantly increased after transfection with pc-*S100A9* compared with the pcDNA3.1 ($P < 0.01$). However, the reverse trend was observed in the si-*S100A9* group (Fig. 3E–3H). Thus, the results discussed in this section showed that *S100A9* increased the release of inflammatory factors and exacerbated cell injury in CPB2 toxin-induced IPEC-J2 cells.

ROS and LDH assays

Cellular ROS levels were measured to investigate further the role of *S100A9* in CPB2 toxin-induced IPEC-J2 cells. The results showed that the fluorescence intensity of the DCFH-DA probe was significantly increased after CPB2 toxin treatment of IPEC-J2 cells
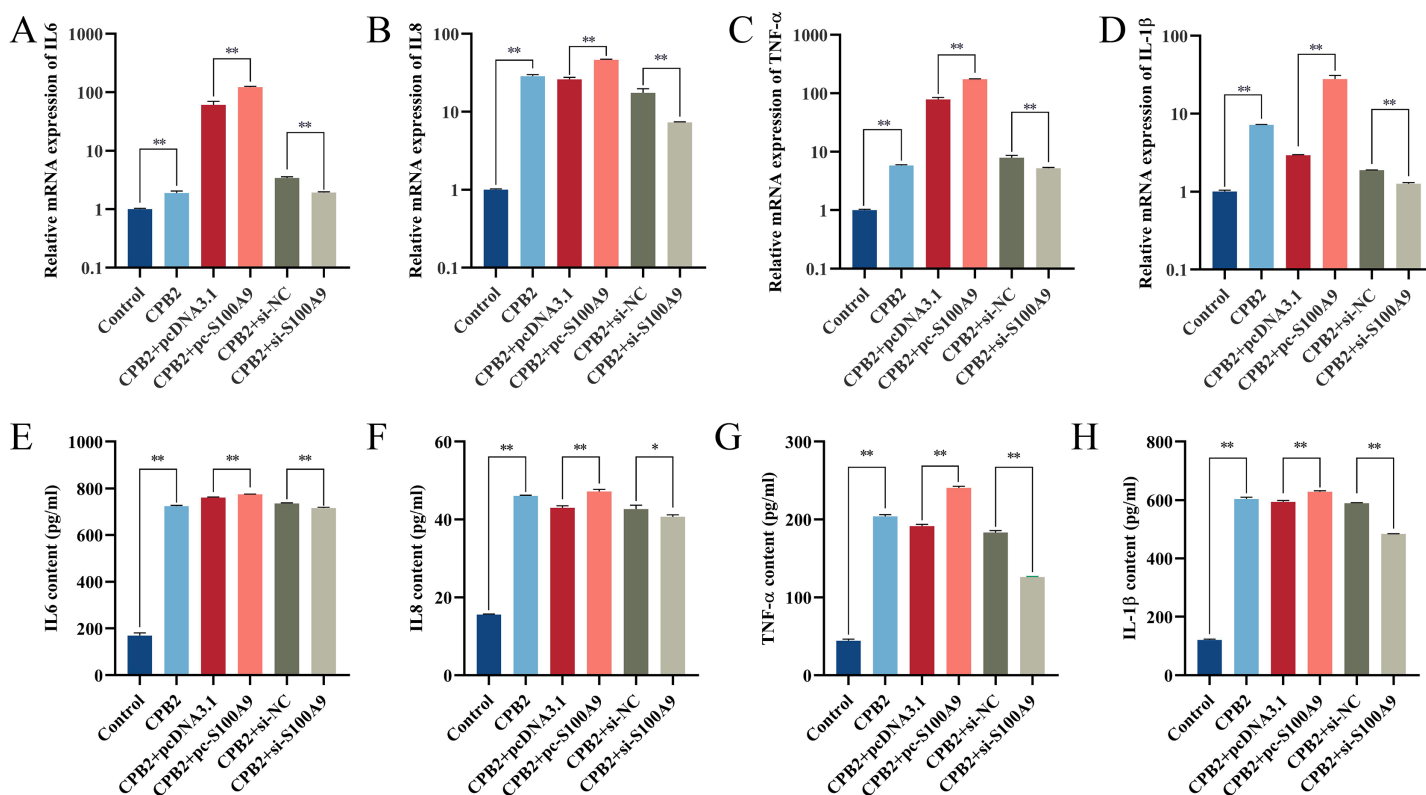
Figure 3 **The effect of *S100A9* on the mRNA expression (A–D) and protein content (E–H) of inflammatory factors induced by CPB2 in IPEC-J2 cells.** $^{*}P < 0.05$, $^{**}P < 0.01$.

compared with the control group ($P < 0.05$). Furthermore, compared with the negative control group, the fluorescence intensity was significantly increased in the *S100A9* overexpression group and significantly decreased in the *S100A9* interference group ($P < 0.01$) (Fig. 4A), indicating that the level of ROS in the cells was elevated after *S100A9* overexpression. Additionally, measurements of the LDH activity cell culture medium revealed that the activity of LDH was significantly increased after CPB2 toxin treatment of IPEC-J2 cells ($P < 0.01$). Furthermore, LDH activity was significantly increased in the *S100A9* overexpression group than in the negative control group. However, the LDH activity was significantly decreased in the *S100A9* interference group ($P < 0.01$) (Fig. 4B). Thus, the results discussed in this section confirmed that *S100A9* promotes cellular damage in CPB2 toxin-induced IPEC-J2 cells.

S100A9 inhibits CPB2-induced IPEC-J2 cell viability and cell proliferation

The CCK-8 assay was used to measure the cell viability to determine the effect of *S100A9* on CPB2 toxin-induced IPEC-J2 cell viability and cell proliferation. The results demonstrated that the cell viability was significantly decreased in the CPB2 group compared to the control group ($P < 0.01$) and significantly decreased in the *S100A9* overexpression group compared to the negative control group ($P < 0.01$). The reverse trend was observed in the *S100A9* interference group (Fig. 5A). The cell proliferation was
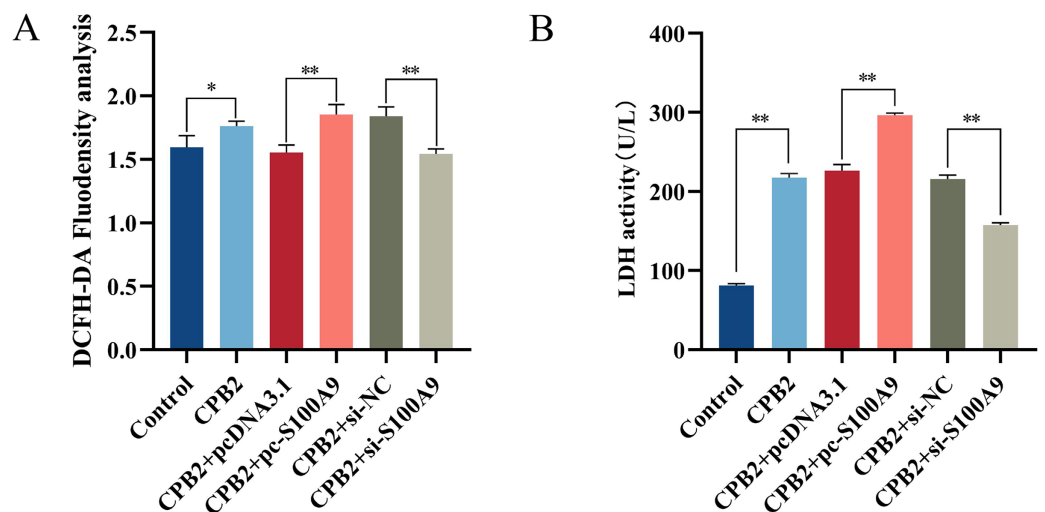
Figure 4 Detection of ROS (A) and LDH (B) in the CPB2 induced IPEC-J2 cells. Stronger fluorescence intensity of the fluorescent probe DCFH-DA implied higher levels of ROS in IPEC-J2 cells. *$P < 0.05$, **$P < 0.01$

detected by the EdU method. The results showed that the number of positive cells in the *S100A9* overexpression group was significantly decreased compared to the negative control group ($P < 0.01$). In contrast, the reverse was observed in the *S100A9* interference group (Fig. 5B). Thus, the results discussed in this section reveal that *S100A9* inhibited cell viability and cell proliferation.

Effect of *S100A9* on the cell cycle of IPEC-J2 cells induced by CPB2 toxin

Flow cytometry analysis was used to determine the proliferation mechanism of *S100A9* in IPEC-J2 cells induced by CPB2 toxin. Figure 6 shows the percentage of cells in each experimental group's G0/G1, G2, and S phases. Compared with the CPB2 group, the percentage of the G0/G1 phase was significantly increased, and the S phase was significantly decreased in the pc-*S100A9* group ($P < 0.01$), while the reverse was observed in the si-*S100A9* group. Thus, the data indicate that the overexpression of *S100A9* prolongs the cell cycle of CPB2 toxin-induced IPEC-J2 cells.

Effect of *S100A9* on tight junction protein expression in CPB2 toxin-induced IPEC-J2 cells

The RT-qPCR assay showed that the expression level of tight junction proteins was significantly decreased in IPEC-J2 cells after exposure to CPB2 toxin ($P < 0.05$). In addition, the expression levels of tight junction proteins *ZO*-1, *OCLN*, and *CLDN*-12 were significantly decreased by the overexpression of *S100A9* in the cells. However, inhibition of *S100A9* expression resulted in the reverse trend ($P < 0.05$) (Fig. 7).
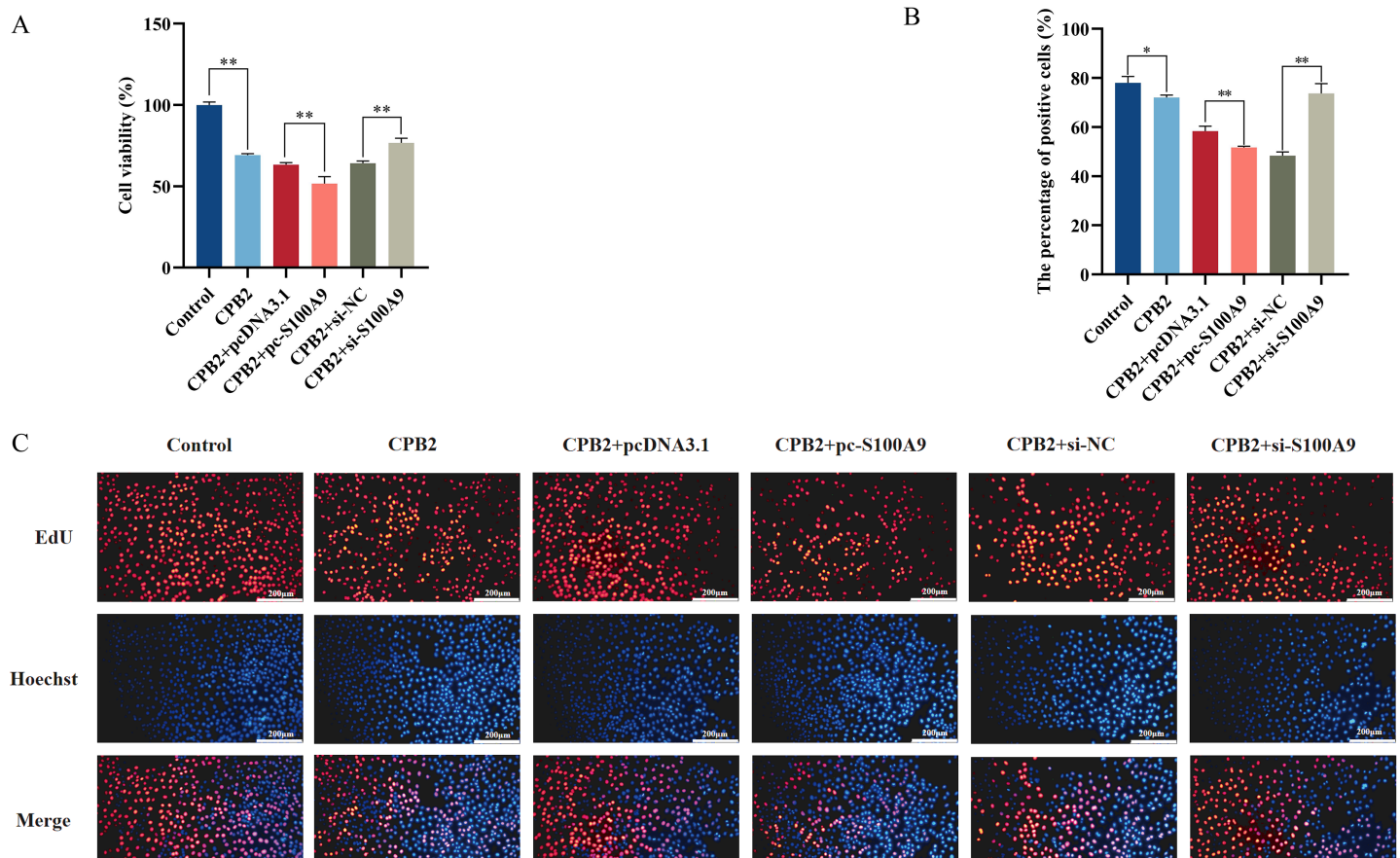
Figure 5 Effect of *S100A9* on CPB2 toxin-induced IPEC-J2 cell viability and proliferation. (A) Cell viability by CCK-8 method. (B) The number of EdU-positive cells. (C) EdU cell proliferation assay. Scale bar: 200 μm. $^{*}P < 0.05$, $^{**}P < 0.01$.

PPI network of immune genes closely related to S100A9

PPI network analysis shows that there were 20 nodes and 222 edges strongly associated with S100A9 (Fig. 8A). The PPI network was analyzed by the MCODE plugin in Cytoscape (V3.8.0) software, and it was found that there were two clusters of proteins in the PPI network that were closely associated with inflammation, one of which contained 15 nodes and 170 edges (Fig. 8B) and was the most critical functional module. The other contained three nodes and six edges (Fig. 8C). The two protein clusters had scores of 12.143 and 3, respectively. In the PPI network, S100A9, S100A8, TLR4, S100A12, ENSSSCP00000027312, TRAF6 and CYBB proteins had higher BC scores of 31.81, 25.36, 20.98, 20.82, 16.34, 15.89, and 13.72, respectively. Among these, S100A9, S100A8, and S100A12 were pro-inflammatory genes, while TLR4, CYBB, CD14, TRAF6, and other genes played a crucial role in regulating the immune response.

DISCUSSION

C. perfringens type C is a Gram-positive anaerobic bacterium that produces the extremely pathogenic CPB2 toxin (*Garcia et al., 2012*), causing a variety of inflammatory reactions and infectious diseases. Newborn piglets are susceptible to infection by CPB2 pathogenic
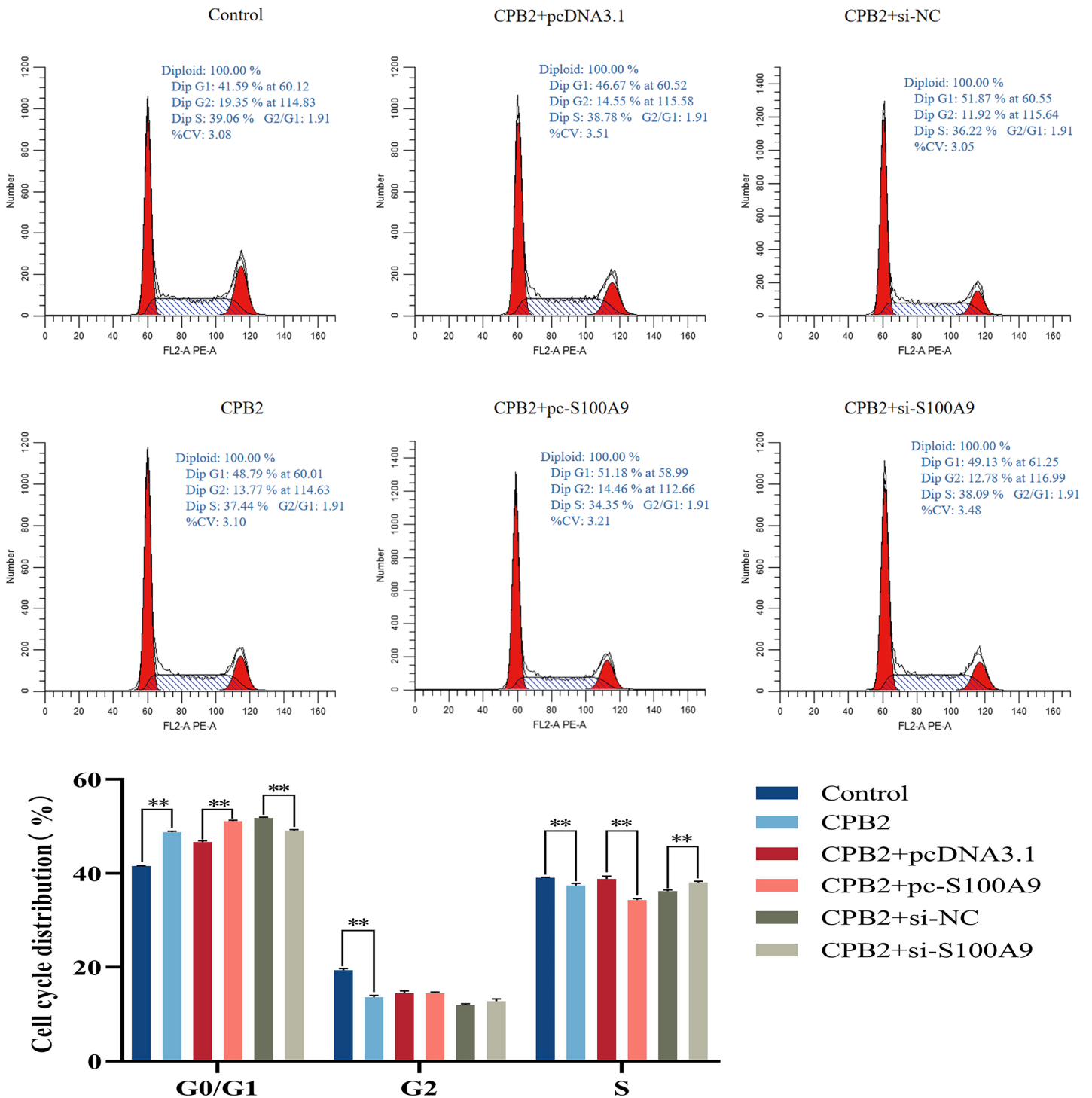
Figure 6 Effects of *S100A9* on the cell cycle of IPEC-J2 cells induced by CPB2 toxin. *$P < 0.05$, **$P < 0.01$.

bacteria, leading to diarrhea, and are the main cause of piglet mortality. At present, it relies mainly on antibiotics and vaccines, but new methods of molecular resistance to the disease need to be explored. It has been previously reported that *S100A9* affected the innate
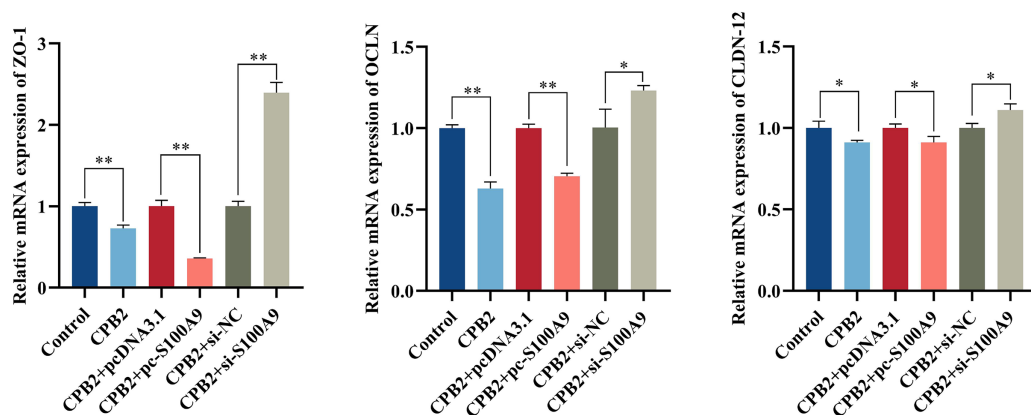
Figure 7 Effects of *S100A9* on CPB2 toxin-induced tight junction protein expression in IPEC-J2 cells. $*P < 0.05$, $**P < 0.01$.

immune response (*Liu et al., 2021*). This study revealed that knockdown of *S100A9* reduced injury due to cellular inflammatory injury suggesting that *S100A9* regulates the progression of diarrheal disease. However, the mechanism of action of *S100A9* in CPB2 toxin-induced diarrhea in piglets is unclear.

S100A9 belongs to the family of damage-associated molecular patterns (DAMPs) (*Ehrchen et al., 2009*), which promote leukocyte aggregation through a positive feedback regulatory mechanism when the body undergoes an inflammatory response and are often used as a reliable marker for a variety of inflammatory diseases, such as psoriasis, cancer, and rheumatoid arthritis (*Christmann et al., 2020*; *Gebhardt et al., 2006*; *Huang et al., 2019a*). *S100A9* is commonly expressed in various cells, such as colonic epithelial cells, macrophages, and cardiomyocytes (*Krenkel et al., 2020*; *Lee et al., 2012*; *Li et al., 2019*). Additionally, multiple studies have reported that the *S100A9* gene is associated with inflammatory diseases, autoimmune disease and infections (*Frohberger et al., 2020*; *Harman et al., 2020*; *Huang et al., 2019a*). The gene is especially involved in triggering and promoting inflammatory responses, pathogenic infections, and toxin-induced lethality, among other processes (*Ehrchen et al., 2009*; *Frohberger et al., 2020*). A study found that increased levels of *S100A9* in inflammatory diseases as a mediator of inflammation and immune response (*Simard et al., 2013*). *Chen et al. (2009)* investigated the effect of *Haemophilus parasuis* (HPS) infection on the transcriptome of pig spleen and found that HPS infection resulted in differential expression of genes such as *S100A8*, *S100A9*, and G protein-coupled receptors, with a 21.8 fold up-regulation of *S100A9* gene expression levels. These genes are involved in regulating signaling pathways such as cellular immune response, apoptosis, and cytokine signaling, and the changes in their activity may lead to HPS inhibiting the recruitment of immune cells, lymphocyte activation, and immune response to immune evasion. Another study demonstrated an increased abundance of *S100A9* expression in the intestine of pigs infected with *Campylobacter jejuni* (*Negretti et al., 2020*). Our study confirmed that the mRNA expression level of *S100A9* was significantly increased in the tissues of piglets susceptible to *C. perfringens* type C. Meanwhile, the expression level of *S100A9* was found to peak at 24 h and then stabilize in
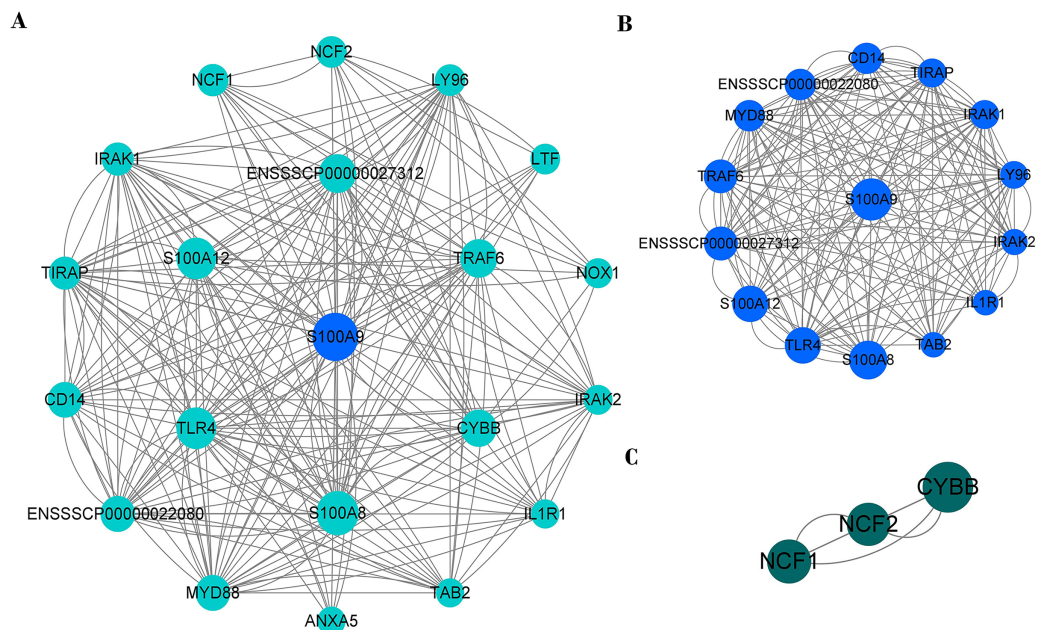
Figure 8 The PPI network of immune genes closely related to S100A9. (A) S100A9 PPI network. (B and C) The main function clusters in the S100A9 PPI network. Larger circles with higher Betweenness Centrality (BC) scores indicate stronger associations with other proteins. A higher number of connecting lines indicate stronger associations.

IPEC-J2 cells treated with CPB2 toxin, indicating that the damage to IPEC-J2 cells by CPB2 toxin results in an increased expression of *S100A9*. The release of *S100A9* may be caused by increased cellular release of inflammatory factors such as *IL6* and *IL8*, which in turn cause a cascade response in the signaling pathway. si-*S100A9* was found to reduce inflammatory damage in dextran sulfate sodium-treated colonic epithelial cells (CEC), and *IL-6* induced *S100A9* expression in CEC through *STAT3* activation *Lee et al. (2012)*, which confirms our research. Recent studies have demonstrated that the *S100A9* gene has an important role in pig resistance to diarrheal diseases caused by bacterial infections. Vectors were transferred into IPEC-J2 by RNA interference and overexpressing cells produced and subsequently treated with CPB2 toxin. It was observed that when the CPB2 toxin injured IPEC-J2, the levels of *IL-6*, *IL8*, *TNF*-α, and *IL-1β* mRNA and concentration were increased. Further, the release of the inflammatory factors was promoted by *S100A9* overexpression, thereby proving that *S100A9* is a key factor in the process of pig diarrheal disease. *Negretti et al. (2020)* used a porcine-ligated loop model to study the porcine intestinal response to *Campylobacter jejuni* infection and found that the abundance of inflammatory cytokines *IL*-8 and *TNF*-α were substantially increased during infection. *Vincent et al. (2015)* used calmodulin in stool as a marker of inflammatory diseases. *S100A9* amplifies inflammatory responses' and plays a key point in the involvement of organisms in immune-related responses (*Vincent et al., 2015*). The ROS levels in the intestine can cause various problems (*Wang et al., 2021*). It has been reported that ROS levels are increased in most inflammatory diseases and that *S100A9* overexpression can result in increased ROS in cells (*Shabani et al., 2018*). In addition, *Zhao et al. (2021)*

investigated the effect of blocking *S100A9* on LPS-induced lung injury in mice and found that the extent of lung injury was reduced after administration of *S100A9*-specific inhibitors in mice. The results of this study show a significant increase in ROS levels in CPB2 toxin-induced IPEC-J2 cells after overexpression of *S100A9*. Further, there was a decrease in ROS levels after inhibition of *S100A9* was inhibited, indicating that the overexpression of *S100A9* exacerbated the cell damage, consistent with previous reports.

LDH is a stable cytoplasmic enzyme present in all cells, and detection of LDH activity in cell culture supernatant is a common method to evaluate cytotoxicity (*Kumar, Nagarajan & Uchil, 2018*; *Sun et al., 2010*) and cell membrane integrity (*da Silva et al., 2019*; *Laev et al., 1993*). LDH release indirectly reflects the degree of cellular damage (*Kumar, Nagarajan & Uchil, 2018*). A previous study found that LDH release was increased in bovine mammary gland epithelial cells induced by *Staphylococcus aureus* (*Zhao et al., 2022*). *Autheman et al. (2013)* did a similar study using rCPB to induce primary porcine endothelial cells. In this study, the enzymatic activity of LDH was examined in the cell culture supernatant of each experimental group. The results revealed a significant increase in LDH activity after overexpression of *S100A9*, with a concomitant decrease in LDH activity after inhibition of *S100A9*; this indicates that cytotoxicity increased and exacerbated cell damage after overexpression of *S100A9*. The cell proliferation and viability were assessed by EdU method and CCK8 method, the overexpression of *S100A9* resulted in the inhibition of cell viability and proliferation of CPB2 toxin-induced IPEC-J2 cells; however, inhibition of *S100A9* had a reverse effect. In addition, there was a significant increase in the percentage of G0/G1 phase cells after the overexpression of *S100A9*, which also indicated that *S100A9* inhibited proliferation of CPB2 toxin-induced IPEC-J2 cells. There exists an extensive literature on the effects of *S100A9* on cell proliferation and apoptosis. *Zheng et al. (2014)* found that *S100A9* has apoptosis-inducing properties on various cells and that recombinant S100A8/9 has stronger apoptosis-inducing activity than *S100A9*. Additionally, calcium-binding proteins is a key enzyme in apoptosis (*Zali et al., 2008*). The consistent with the results of our study.

Tight junction proteins are known to be closely related to cellular permeability. It has been found that the level of *ZO-1* is significantly reduced when the inflammatory response occurs in the lung, and the PDZ structural domain regulates the LPS-induced inflammatory response in *ZO-1* (*Lee, Choi & Song, 2020*). Also, tight junction proteins are involved in various intestinal diseases, and their deletion can cause intestinal epithelial dysfunction. Thus, the tight junction proteins play a crucial role in regulating the inflammatory response of the body (*Jiang et al., 2021*), consistent with our findings. We found that the overexpression of *S100A9* promoted CPB2 toxin-induced injury in IPEC-J2 cells, resulting in a significant decrease in the expression of tight junction proteins. Protein-protein interaction facilitates the functioning, and the prediction of PPI networks is critical for our understanding of biological functions and interactions between cellular components (*Athanasios et al., 2017*). With the development of various histological techniques, molecular PPI network predictions are becoming more reliable and can predict several diseases by constructing disease models (*Tomkins & Manzoni, 2021*). The immune response can be predicted based on protein-protein interactions (*Mizoguchi & Mizoguchi,*

2007). Previous studies have shown that *S100A9* binds to various proteins to regulate immune responses (*Björk et al., 2009*). The S100A9 has been shown to be a ligand for TLR4 (*Björk et al., 2009*). TLR4 is expressed in IPEC-J2 cells (*Burkey et al., 2009*). It was found that *S100A9* could bind to TLR4 to regulate inflammatory response (*Raymond et al., 2014*). In our study, there was a stronger role between S100A9 and TLR4, which could be another mechanism by which S100A9 exacerbates cell injury, but needs to be verified by further experiments. In addition, TLR4 has been shown to interact with *TIRAP*, *CD14*, and *MyD88* to mediate LPS-induced innate immune responses (*Tatematsu et al., 2016*). TRAF6 has been reported to mediate various protein-protein interactions that can activate NF-κB and MAPK pathways to regulate immune responses (*Walsh, Lee & Choi, 2015*). Additionally, due to genetic variants, deletions of *NCF1*, *NCF2*, and *CYBB* can cause hereditary immune diseases (*O'Neill et al., 2015*). In this study, we constructed a PPI network of S100A9 with other proteins and identified a cluster of proteins, with a score of 12.143, that might play an important role in the inflammatory response.

CONCLUSIONS

In conclusion, this study confirmed that the *S100A9* gene promoted inflammatory injury in CPB2 toxin-induced IPEC-J2 cells, inhibited cellular proliferation, and disrupted cellular tight junctions. Our study revealed the molecular mechanism by which *S100A9* regulates CPB2 toxin-induced IPEC-J2 cell damage.

ACKNOWLEDGEMENTS

The authors would like to thank all the reviewers who participated in the review, as well as MJEditor for providing English editing services during the preparation of this manuscript. We gratefully acknowledge all the other members work in Animal Genetics Breeding and Reproduction Laboratory for their kind help during experiments.

Funding

This work was supported by the Higher Education Innovation Fund of Gansu Province (2022B-106), the National Natural Science Foundation of China (31960646), the Youth Science and Technology Fund Program of Gansu Province (20JR5RA005), and the Protection and Quality Improvement of Gansu Local Pig Germplasm Resources (GSLK-2021-13). The funders had no role in study design, data collection and analysis, decision to publish, or preparation of the manuscript.

Grant Disclosures

The following grant information was disclosed by the authors:
Higher Education Innovation Fund of Gansu Province: 2022B-106.
National Natural Science Foundation of China: 31960646.
Youth Science and Technology Fund Program of Gansu Province: 20JR5RA005.

Protection and Quality Improvement of Gansu Local Pig Germplasm Resources: GSLK-2021-13.

Competing Interests
The authors declare that they have no competing interests.

Author Contributions
- Jie Li conceived and designed the experiments, performed the experiments, analyzed the data, prepared figures and/or tables, authored or reviewed drafts of the article, and approved the final draft.
- Xiaoyu Huang conceived and designed the experiments, authored or reviewed drafts of the article, and approved the final draft.
- Kaihui Xie performed the experiments, prepared figures and/or tables, and approved the final draft.
- Juanli Zhang analyzed the data, prepared figures and/or tables, and approved the final draft.
- Jiaojiao Yang performed the experiments, prepared figures and/or tables, and approved the final draft.
- Zunqiang Yan analyzed the data, prepared figures and/or tables, and approved the final draft.
- Shuangbao Gun conceived and designed the experiments, authored or reviewed drafts of the article, and approved the final draft.

Animal Ethics
The following information was supplied relating to ethical approvals (*i.e.*, approving body and any reference numbers):

The research was approved by the Institutional Ethic Committee of Gansu Agricultural University (Approval No. GAU-LC-2018-054).

Data Availability
Raw data are available in the Supplemental Files and Figshare:

Li, Jie (2022): Decreased S100A9 expression alleviates *Clostridium perfringens* beta2 toxin-induced inflammatory injury in IPEC-J2 cells. figshare. Dataset. https://doi.org/10.6084/m9.figshare.21225776.v1.

Supplemental Information
Supplemental information for this article can be found online at http://dx.doi.org/10.7717/peerj.14722#supplemental-information.

REFERENCES
Abers MS, Delmonte OM, Ricotta EE, Fintzi J, Fink DL, de Jesus AAA, Zarember KA, Alehashemi S, Oikonomou V, Desai JV, Canna SW, Shakoory B, Dobbs K, Imberti L, Sottini A, Quiros-Roldan E, Castelli F, Rossi C, Brugnoni D, Biondi A, Bettini LR, D'Angio M, Bonfanti P, Castagnoli R, Montagna D, Licari A, Marseglia GL, Gliniewicz EF,

Shaw E, Kahle DE, Rastegar AT, Stack M, Myint-Hpu K, Levinson SL, DiNubile MJ, Chertow DW, Burbelo PD, Cohen JI, Calvo KR, Tsang JS, Su HC, Gallin JI, Kuhns DB, Goldbach-Mansky R, Lionakis MS, Notarangelo LD. 2021. An immune-based biomarker signature is associated with mortality in COVID-19 patients. *JCI Insight* **6**(1):e144455 DOI 10.1172/jci.insight.144455.

Athanasios A, Charalampos V, Vasileios T, Ashraf GM. 2017. Protein-Protein Interaction (PPI) network: recent advances in drug discovery. *Current Drug Metabolism* **18**(1):5–10 DOI 10.2174/138920021801170119204832.

Autheman D, Wyder M, Popoff M, D'Herde K, Christen S, Posthaus H. 2013. *Clostridium perfringens* beta-toxin induces necrostatin-inhibitable, calpain-dependent necrosis in primary porcine endothelial cells. *PLOS ONE* **8**(5):e64644 DOI 10.1371/journal.pone.0064644.

Björk P, Björk A, Vogl T, Stenström M, Liberg D, Olsson A, Roth J, Ivars F, Leanderson T. 2009. Identification of human S100A9 as a novel target for treatment of autoimmune disease via binding to quinoline-3-carboxamides. *PLOS Biology* **7**(4):e97 DOI 10.1371/journal.pbio.1000097.

Brosnahan AJ, Brown DR. 2012. Porcine IPEC-J2 intestinal epithelial cells in microbiological investigations. *Veterinary Microbiology* **156**(3–4):229–237 DOI 10.1016/j.vetmic.2011.10.017.

Burkey TE, Skjolaas KA, Dritz SS, Minton JE. 2009. Expression of porcine toll-like receptor 2, 4 and 9 gene transcripts in the presence of lipopolysaccharide and *Salmonella enterica* serovars Typhimurium and Choleraesuis. *Veterinary Immunology and Immunopathology* **130**(1–2):96–101 DOI 10.1016/j.vetimm.2008.12.027.

Chen H, Li C, Fang M, Zhu M, Li X, Zhou R, Li K, Zhao S. 2009. Understanding *Haemophilus parasuis* infection in porcine spleen through a transcriptomics approach. *BMC Genomics* **10**(1):64 DOI 10.1186/1471-2164-10-64.

Christmann C, Zenker S, Martens L, Hübner J, Loser K, Vogl T, Roth J. 2020. Interleukin 17 promotes expression of alarmins S100A8 and S100A9 during the inflammatory response of keratinocytes. *Frontiers in Immunology* **11**:599947 DOI 10.3389/fimmu.2020.599947.

da Silva PCS, Marques NP, Farina MT, Oliveira TM, Duque C, Marques NCT, Sakai VT. 2019. Laser treatment contributes to maintain membrane integrity in stem cells from human exfoliated deciduous teeth (shed) under nutritional deficit. *Lasers In Medical Science* **34**(1):15–21 DOI 10.1007/s10103-018-2574-x.

Darweesh MF, Rajput MKS, Braun LJ, Rohila JS, Chase CCL. 2018. BVDV Npro protein mediates the BVDV induced immunosuppression through interaction with cellular S100A9 protein. *Microbial Pathogenesis* **121**(11):341–349 DOI 10.1016/j.micpath.2018.05.047.

Ehrchen JM, Sunderkötter C, Foell D, Vogl T, Roth J. 2009. The endogenous toll-like receptor 4 agonist S100A8/S100A9 (calprotectin) as innate amplifier of infection, autoimmunity, and cancer. *Journal of Leukocyte Biology* **86**(3):557–566 DOI 10.1189/jlb.1008647.

Forti K, Ferroni L, Pellegrini M, Cruciani D, De Giuseppe A, Crotti S, Papa P, Maresca C, Severi G, Marenzoni ML, Cagiola M. 2020. Molecular characterization of *Clostridium perfringens* strains isolated in Italy. *Toxins* **12**(10):650 DOI 10.3390/toxins12100650.

Frohberger SJ, Fercoq F, Neumann A-L, Surendar J, Stamminger W, Ehrens A, Karunakaran I, Remion E, Vogl T, Hoerauf A, Martin C, Hübner MP. 2020. S100A8/S100A9 deficiency increases neutrophil activation and protective immune responses against invading infective L3 larvae of the filarial nematode litomosoides sigmodontis. *PLOS Neglected Tropical Diseases* **14**(2):e0008119 DOI 10.1371/journal.pntd.0008119.

Gan Y, Zheng S, Baak JPA, Zhao S, Zheng Y, Luo N, Liao W, Fu C. 2015. Prediction of the anti-inflammatory mechanisms of curcumin by module-based protein interaction network analysis. *Acta Pharmaceutica Sinica B* **5(6)**:590–595 DOI 10.1016/j.apsb.2015.09.005.

Gao X, Yang Q, Huang X, Yan Z, Zhang S, Luo R, Wang P, Wang W, Xie K, Jiang T, Gun S. 2020. Effects of *Clostridium perfringens* beta2 toxin on apoptosis, inflammation, and barrier function of intestinal porcine epithelial cells. *Microbial Pathogenesis* **147**:104379 DOI 10.1016/j.micpath.2020.104379.

Garcia JP, Beingesser J, Fisher DJ, Sayeed S, McClane BA, Posthaus H, Uzal FA. 2012. The effect of *Clostridium perfringens* type C strain CN3685 and its isogenic beta toxin null mutant in goats. *Veterinary Microbiology* **157(3–4)**:412–419 DOI 10.1016/j.vetmic.2012.01.005.

Gebhardt C, Németh J, Angel P, Hess J. 2006. S100A8 and S100A9 in inflammation and cancer. *Biochemical Pharmacology* **72(11)**:1622–1631 DOI 10.1016/j.bcp.2006.05.017.

Gibert M, Jolivet-Reynaud C, Popoff MR, Jolivet-Renaud C. 1997. Beta2 toxin, a novel toxin produced by *Clostridium perfringens*. *Gene* **203(1)**:65–73 DOI 10.1016/S0378-1119(97)00493-9.

Gurtner C, Popescu F, Wyder M, Sutter E, Zeeh F, Frey J, von Schubert C, Posthaus H. 2010. Rapid cytopathic effects of *Clostridium perfringens* beta-toxin on porcine endothelial cells. *Infection and Immunity* **78(7)**:2966–2973 DOI 10.1128/IAI.01284-09.

Harman JL, Loes AN, Warren GD, Heaphy MC, Lampi KJ, Harms MJ. 2020. Evolution of multifunctionality through a pleiotropic substitution in the innate immune protein S100A9. *ELife* **9**:e54100 DOI 10.7554/eLife.54100.

Huang X, Sun W, Yan Z, Shi H, Yang Q, Wang P, Li S, Liu L, Zhao S, Gun S. 2019b. Integrative analyses of long non-coding RNA and mRNA involved in piglet ileum immune response to type C infection. *Frontiers in Cellular and Infection Microbiology* **9**:130 DOI 10.3389/fcimb.2019.00130.

Huang XY, Sun WY, Yan ZQ, Shi HR, Yang QL, Wang PF, Li SG, Liu LX, Zhao SG, Gun SB. 2019c. Novel insights reveal anti-microbial gene regulation of piglet intestine immune in response to *Clostridium perfringens* infection. *Scientific Reports* **9(1)**:1963 DOI 10.1038/s41598-018-37898-5.

Huang M, Wu R, Chen L, Peng Q, Li S, Zhang Y, Zhou L, Duan L. 2019a. S100A9 regulates MDSCs-mediated immune suppression via the RAGE and TLR4 signaling pathways in colorectal carcinoma. *Frontiers in Immunology* **10**:2243 DOI 10.3389/fimmu.2019.02243.

Jhang KA, Lee EO, Kim H-S, Chang K-A, Suh Y-H, Chong YH. 2016. S100A9 exacerbates the Aβ1-42-mediated innate immunity in human THP-1 monocytes. *CNS & Neurological Disorders-Drug Targets* **15(8)**:910–917 DOI 10.2174/1871527315666160815161922.

Jiang Y, Song J, Xu Y, Liu C, Qian W, Bai T, Hou X. 2021. Piezo1 regulates intestinal epithelial function by affecting the tight junction protein claudin-1 via the ROCK pathway. *Life Sciences* **275(12)**:119254 DOI 10.1016/j.lfs.2021.119254.

Källberg E, Vogl T, Liberg D, Olsson A, Björk P, Wikström P, Bergh A, Roth J, Ivars F, Leanderson T. 2012. S100A9 interaction with TLR4 promotes tumor growth. *PLOS ONE* **7**:e34207 DOI 10.1371/journal.pone.0034207.

Krenkel O, Hundertmark J, Abdallah AT, Kohlhepp M, Puengel T, Roth T, Branco DPP, Mossanen JC, Luedde T, Trautwein C, Costa IG, Tacke F. 2020. Myeloid cells in liver and bone marrow acquire a functionally distinct inflammatory phenotype during obesity-related steatohepatitis. *Gut* **69(3)**:551–563 DOI 10.1136/gutjnl-2019-318382.

Kumar P, Nagarajan A, Uchil PD. 2018. Analysis of cell viability by the lactate dehydrogenase assay. *Cold Spring Harbor Protocols* **6**:465–468 DOI 10.1101/pdb.prot095497.

Kwon CH, Moon HJ, Park HJ, Choi JH, Park DY. 2013. S100A8 and S100A9 promotes invasion and migration through p38 mitogen-activated protein kinase-dependent NF-κB activation in gastric cancer cells. *Molecules and Cells* **35(3)**:226–234 DOI 10.1007/s10059-013-2269-x.

Laev H, Mahadik SP, Bonheur JL, Hernandez N, Karpiak SE. 1993. GM1 ganglioside reduces glutamate toxicity to cortical cells. Lowered LDH release and preserved membrane integrity. *Molecular and Chemical Neuropathology* **20(3)**:229–243 DOI 10.1007/BF03160076.

Lee T-H, Chang HS, Bae D-J, Song HJ, Kim M-S, Park JS, Jun JA, Lee SY, Uh ST, Kim SH, Park C-S. 2017. Role of S100A9 in the development of neutrophilic inflammation in asthmatics and in a murine model. *Clinical Immunology (Orlando, Fla)* **183**:158–166 DOI 10.1016/j.clim.2017.08.013.

Lee TJ, Choi YH, Song KS. 2020. The PDZ motif peptide of ZO-1 attenuates *Pseudomonas aeruginosa* LPS-induced airway inflammation. *Scientific Reports* **10(1)**:19644 DOI 10.1038/s41598-020-76883-9.

Lee MJ, Lee J-K, Choi JW, Lee C-S, Sim JH, Cho C-H, Lee K-H, Cho I-H, Chung M-H, Kim H-R, Ye S-K. 2012. Interleukin-6 induces S100A9 expression in colonic epithelial cells through STAT3 activation in experimental ulcerative colitis. *PLOS ONE* **7(9)**:e38801 DOI 10.1371/journal.pone.0038801.

Li Y, Chen B, Yang X, Zhang C, Jiao Y, Li P, Liu Y, Li Z, Qiao B, Bond Lau W, Ma X-L, Du J. 2019. S100a8/a9 signaling causes mitochondrial dysfunction and cardiomyocyte death in response to ischemic/reperfusion injury. *Circulation* **140(9)**:751–764 DOI 10.1161/CIRCULATIONAHA.118.039262.

Liu Q, Li R, Li Q, Luo B, Lin J, Lyu L. 2021. High levels of plasma S100A9 at admission indicate an increased risk of death in severe tuberculosis patients. *Journal of Clinical Tuberculosis and Other Mycobacterial Diseases* **25(1)**:100270 DOI 10.1016/j.jctube.2021.100270.

Liu F, Li G, Wen K, Bui T, Cao D, Zhang Y, Yuan L. 2010. Porcine small intestinal epithelial cell line (IPEC-J2) of rotavirus infection as a new model for the study of innate immune responses to rotaviruses and probiotics. *Viral Immunology* **23(2)**:135–149 DOI 10.1089/vim.2009.0088.

Livak KJ, Schmittgen TD. 2001. Analysis of relative gene expression data using real-time quantitative PCR and the 2(-Delta Delta C(T)) method. *Methods (San Diego, Calif)* **25(4)**:402–408 DOI 10.1006/meth.2001.1262.

Luo R, Yang Q, Huang X, Yan Z, Gao X, Wang W, Xie K, Wang P, Gun S. 2020. *Clostridium perfringens* beta2 toxin induced in vitro oxidative damage and its toxic assessment in porcine small intestinal epithelial cell lines. *Gene* **759**:144999 DOI 10.1016/j.gene.2020.144999.

Markowitz J, Carson WE. 2013. Review of S100A9 biology and its role in cancer. *Biochimica et Biophysica Acta (BBA)-Reviews on Cancer* **1835(1)**:100–109 DOI 10.1016/j.bbcan.2012.10.003.

Mizoguchi E, Mizoguchi A. 2007. Is the sugar always sweet in intestinal inflammation? *Immunologic Research* **37(1)**:47–60 DOI 10.1007/BF02686089.

Nagahama M, Hayashi S, Morimitsu S, Sakurai J. 2003. Biological activities and pore formation of *Clostridium perfringens* beta toxin in HL 60 cells. *The Journal of Biological Chemistry* **278(38)**:36934–36941 DOI 10.1074/jbc.M306562200.

Nagahama M, Ochi S, Oda M, Miyamoto K, Takehara M, Kobayashi K. 2015. Recent insights into *Clostridium perfringens* beta-toxin. *Toxins* **7(2)**:396–406 DOI 10.3390/toxins7020396.

Negretti NM, Ye Y, Malavasi LM, Pokharel SM, Huynh S, Noh S, Klima CL, Gourley CR, Ragle CA, Bose S, Looft T, Parker CT, Clair G, Adkins JN, Konkel ME. 2020. A porcine ligated loop model reveals new insight into the host immune response against *Campylobacter jejuni*. *Gut Microbes* **12(1)**:1814121 DOI 10.1080/19490976.2020.1814121.

O'Neill S, Brault J, Stasia M-J, Knaus UG. 2015. Genetic disorders coupled to ROS deficiency. *Redox Biology* **6**(375–382):135–156 DOI 10.1016/j.redox.2015.07.009.

Pandolfi F, Altamura S, Frosali S, Conti P. 2016. Key role of DAMP in inflammation, cancer, and tissue repair. *Clinical Therapeutics* **38**(5):1017–1028 DOI 10.1016/j.clinthera.2016.02.028.

Posthaus H, Kittl S, Tarek B, Bruggisser J. 2020. Type C necrotic enteritis in pigs: diagnosis, pathogenesis, and prevention. *Journal of Veterinary Diagnostic Investigation: Official Publication of the American Association of Veterinary Laboratory Diagnosticians, Inc* **32**(2):203–212 DOI 10.1177/1040638719900180.

Raymond E, Dalgleish A, Damber JE, Smith M, Pili R. 2014. Mechanisms of action of tasquinimod on the tumour microenvironment. *Cancer Chemotherapy and Pharmacology* **73**(1):1–8 DOI 10.1007/s00280-013-2321-8.

Schumacher VL, Martel A, Pasmans F, Van Immerseel F, Posthaus H. 2013. Endothelial binding of beta toxin to small intestinal mucosal endothelial cells in early stages of experimentally induced *Clostridium perfringens* type C enteritis in pigs. *Veterinary Pathology* **50**(4):626–629 DOI 10.1177/0300985812461362.

Shabani F, Farasat A, Mahdavi M, Gheibi N. 2018. Calprotectin (S100A8/S100A9): a key protein between inflammation and cancer. *Inflammation research: Official Journal of the European Histamine Research Society* **67**(10):801–812 DOI 10.1007/s00011-018-1173-4.

Simard J-C, Cesaro A, Chapeton-Montes J, Tardif M, Antoine F, Girard D, Tessier PA. 2013. S100A8 and S100A9 induce cytokine expression and regulate the NLRP3 inflammasome via ROS-dependent activation of NF-κB(1.). *PLOS ONE* **8**(8):e72138 DOI 10.1371/journal.pone.0072138.

Sun Z-W, Zhang L, Zhu S-J, Chen W-C, Mei B. 2010. Excitotoxicity effects of glutamate on human neuroblastoma SH-SY5Y cells via oxidative damage. *Neuroscience Bulletin* **26**:8–16 DOI 10.1007/s12264-010-0813-7.

Tatematsu M, Yoshida R, Morioka Y, Ishii N, Funami K, Watanabe A, Saeki K, Seya T, Matsumoto M. 2016. Raftlin controls lipopolysaccharide-induced TLR4 internalization and TICAM-1 signaling in a cell type-specific manner. *Journal of Immunology (Baltimore, Md: 1950)* **196**(9):3865–3876 DOI 10.4049/jimmunol.1501734.

Tomkins JE, Manzoni C. 2021. Advances in protein-protein interaction network analysis for Parkinson's disease. *Neurobiology of Disease* **155**(Suppl):105395 DOI 10.1016/j.nbd.2021.105395.

Uzal FA, Vidal JE, McClane BA, Gurjar AA. 2010. *Clostridium perfringens* toxins involved in mammalian veterinary diseases. *The Open Toxinology Journal* **2**:24–42 DOI 10.2174/1875414701003020024.

van Asten AJAM, Nikolaou GN, Gröne A. 2010. The occurrence of cpb2-toxigenic *Clostridium perfringens* and the possible role of the beta2-toxin in enteric disease of domestic animals, wild animals and humans. *Veterinary Journal (London, England: 1997)* **183**(2):135–140 DOI 10.1016/j.tvjl.2008.11.005.

Vincent Z, Hornby S, Ball S, Sanders G, Ayling RM. 2015. Faecal calprotectin as a marker for oesophago-gastric cancer. *Annals of Clinical Biochemistry* **52**(6):660–664 DOI 10.1177/0004563215578191.

Vogl T, Tenbrock K, Ludwig S, Leukert N, Ehrhardt C, van Zoelen MAD, Nacken W, Foell D, van der Poll T, Sorg C, Roth J. 2007. Mrp8 and Mrp14 are endogenous activators of toll-like receptor 4, promoting lethal, endotoxin-induced shock. *Nature Medicine* **13**(9):1042–1049 DOI 10.1038/nm1638.
Walsh MC, Lee J, Choi Y. 2015. Tumor necrosis factor receptor- associated factor 6 (TRAF6) regulation of development, function, and homeostasis of the immune system. *Immunological Reviews* **266(1)**:72–92 DOI 10.1111/imr.12302.

Wang L, Shi Z, Wang X, Mu S, Xu X, Shen L, Li P. 2021. Protective effects of bovine milk exosomes against oxidative stress in IEC-6 cells. *European Journal of Nutrition* **60(1)**:317–327 DOI 10.1007/s00394-020-02242-z.

Yang QL, Kong JJ, Wang DW, Zhao SG, Gun SB. 2013. Swine leukocyte antigen-DQA gene variation and its association with piglet diarrhea in large white, landrace and duroc. *Asian-Australasian Journal of Animal Sciences* **26(8)**:1065–1071 DOI 10.5713/ajas.2013.13067.

Zali H, Rezaei-Tavirani M, Kariminia A, Yousefi R, Shokrgozar MA. 2008. Evaluation of growth inhibitory and apoptosis inducing activity of human calprotectin on the human gastric cell line (AGS). *Iranian Biomedical Journal* **12(7)**:7–14 DOI 10.1016/0730-725X(95)00047-K.

Zhao B, Lu R, Chen J, Xie M, Zhao X, Kong L. 2021. S100A9 blockade prevents lipopolysaccharide-induced lung injury via suppressing the NLRP3 pathway. *Respiratory Research* **22(1)**:45 DOI 10.1186/s12931-021-01641-y.

Zhao Y, Tang J, Yang D, Tang C, Chen J. 2022. Corrigendum to "Staphylococcal enterotoxin M induced inflammation and impairment of bovine mammary epithelial cells" (J. Dairy Sci. 103:8350-8359). *Journal of Dairy Science* **103(8)**:8350–8359 DOI 10.3168/jds.2022-105-8-7140.

Zheng Y, Hou J, Peng L, Zhang X, Jia L, Wang X, Wei S, Meng H. 2014. The pro-apoptotic and pro-inflammatory effects of calprotectin on human periodontal ligament cells. *PLOS ONE* **9(10)**:e110421 DOI 10.1371/journal.pone.0110421.